Aalborg Universitet

AALBORG UNIVERSITY
DENMARK

Prediction of Seismic Damage-Based Degradation in RC Structures

Kirkegaard, Poul Henning; Gupta, Vinay K. ; Nielsen, Søren R.K.

[Link to publication from Aalborg University](#)

Prediction of Seismic Damage-Based Degradation in RC Structures

V.K. Gupta, S.R.K. Nielsen & P.H. Kirkegaard
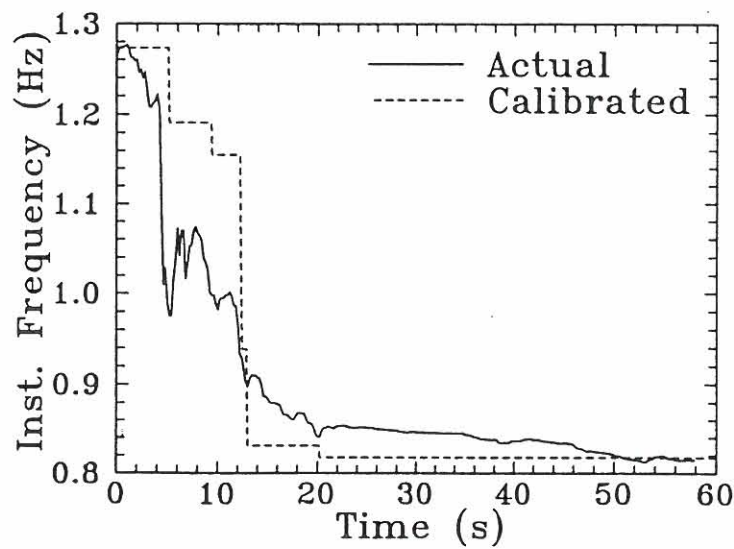
PREDICTION OF SEISMIC DAMAGE-BASED DEGRADATION IN RC STRUCTURES

Vinay K. Gupta
Dept. of Civil Engg., IIT Kanpur, India

Søren R.K. Nielsen and Poul H. Kirkegaard
Dept. of Building Technology & Structural Engg., Aalborg University, Denmark

SUMMARY

Estimation of structural damage from known increase in the fundamental period of a structure after an earthquake or prediction of degradation of stiffness and strength for known damage requires reliable correlations between these response functionals. This study proposes a modified Clough-Johnston SDOF oscillator to establish these correlations in case of a simple elasto-plastic oscillator. It is assumed that the oscillator closely describes the response of a given multi-degree-of-freedom system in its fundamental mode throughout the duration of the excitation. The proposed model considers the design yield strength and ductility supply as two input parameters which must be estimated over a narrow range of ductility supply from a frequency degradation curve. This curve is to be identified from a set of recorded excitation and response time-histories. The proposed model has been used to obtain useful correlations of strength and stiffness degradation with damage wherein a simple damage parameter based on maximum and yield displacements and ductility supply ratio has been considered. The proposed model has also been used to demonstrate that ignoring aftershocks in case of impulsive ground motions may lead to unsafe designs.

INTRODUCTION

Damage caused by earthquakes to the reinforced concrete structures usually results in the stiffness and strength deterioration of the whole structure. This often forms the basis for making suitable repair decisions for the partly damaged structure where the damage is not so obvious. In such cases, the recorded excitation and response time-histories during the last earthquake event are used, if those are available, for reliable post-earthquake estimation of local and global damage in the structure (e.g., see Köylüoğlu et al. (1997)). In those situations where such recorded time series are not available, one may directly measure the change in the natural period of the structure through ambient vibration testing. Damage can then be estimated in terms of the degradation in the structural stiffness, provided reliable correlation of damage with relative stiffness degradation is available. Such correlations are also required when changed properties of the structure are needed to make future reliability estimates while estimated damage through inspection is the only information available. Similar situation arises when one wishes to make his design decision by estimat-

1

CALIBRATION OF THE MODEL

Since the proposed model is to be used for the estimation of structural damage, its calibration should preferably be damage-based. In order to estimate damage during an earthquake, it is considered convenient to identify the instantaneous frequency, $\omega(t)$, of the structure (in its first mode) from the excitation and response time-histories and to see how this is decreased from the initial value of ω_0 to a lower value at the end of the excitation (Di-Pasquale and Çakmak (1990)). This degradation curve of the instantaneous frequency can form the basis for the damage-based calibration of the proposed model. For this purpose, the instantaneous frequency of the above SDOF oscillator during a cycle may be estimated by considering an equivalent linear oscillator and by comparing the average slope of the hysteretic loop (which is the slope of the line through the extreme points of unloading) with the original value of unity. Thus, the expression for the estimated frequency becomes (Köylüoğlu et al. (1997)),

$$\omega(t) = \omega_0 \sqrt{\frac{2z_0(t)}{2z_0(t) + D(t)}} \, . \tag{6}$$

Though the matching of actual and estimated frequency degradation curves may be carried out through iterations over both z_{00} and n, it may be proper to fix the value of n to a realistic level (as it is a measure of ductility available with the system) and then to calibrate the value of z_{00}.
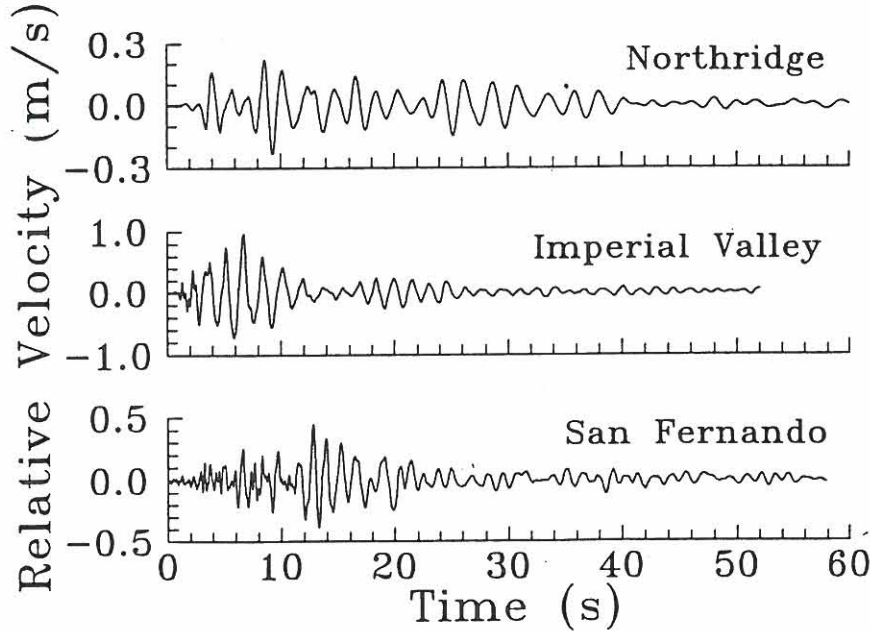

Figure 2 *Relative Velocity Time-Histories Recorded during the Three Example Earthquake Events.*

4

Calibration of the proposed model has been carried out in three cases of recorded floor accelerograms: (i) 7-story hotel at 8244 Orion Boulevard, Van Nuys, California, during the 1994 Northridge earthquake, (ii) Imperial County Services Building, El Centro, California, during the 1979 Imperial Valley earthquake, and (iii) same building as in (i), during the 1971 San Fernando earthquake. The records in all three cases were taken from the sensors placed at the ground floors and roofs in the east-west direction. The identification of the instantaneous natural frequency has been performed on the relative velocity time-history in each case (as shown in Fig. 2) by using a Recursive Auto-Regressive Moving-Average (RARMAX) model (Kirkegaard et al. (1996)). This identification technique can detect time varying characteristics at each time step and is therefore suitable for identifying the
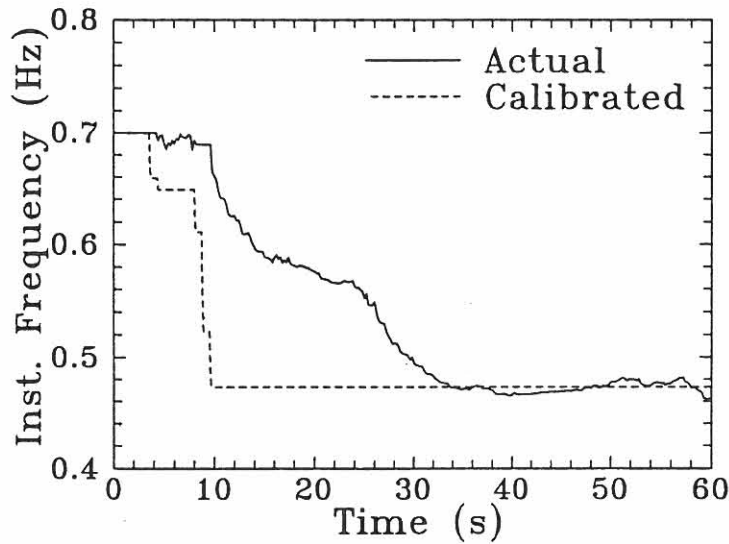

Figure 3 *Comparison of Actual (Identified) and Calibrated Variations of Instantaneous Frequency with Time during the Northridge Earthquake.*

time-varying systems. For each of the considered time series, the model orders of the RARMAX model have been determined by using different model selection criteria such as Akaike's information criterion and pole plots etc. RARMAX models with 6–12 AR parameters have been used for different time-histories. Frequency degradation curves as identified from the time-histories of Fig. 2 are shown in Figs. 3, 4 and 5 respectively. Calibration of the model has been done for $n = 4$, 6 and 8 in each case, and the values of z_{00} so obtained are given in Table 1. The natural frequency, ω_0, of each undamaged structure is also given in this table. Figs. 3–5 also show the frequency degradation curves as obtained from the calibrated models for $n = 6$. It may be seen that these curves are in good matching with the actual curves in the beginning and at the end of the excitation for all three cases. Overall matching during the excitation is also reasonably acceptable considering that only one parameter has been allowed to vary for the calibration and that we are primarily interested in accurately modelling final effect of the ground motion on

5

Table 1 – Identified Natural Frequency, ω_0, and Calibrated Values of z_{00} for Example Earthquake Events

Earthquake Event	ω_0 (rad/s)	z_{00} (m)		
		$n = 4$	$n = 6$	$n = 8$
Northridge	4.398	0.034	0.0316	0.030
Imperial Valley	6.409	0.129	0.122	0.118
San Fernando	7.998	0.042	0.039	0.037

DAMAGE-BASED STIFFNESS AND STRENGTH DEGRADATION

Though several models have been proposed in the recent past to provide a quantitative measure of the structural damage, the model proposed by Park and Ang (1985) has been most widely used and calibrated against actually observed damage states. According to this model, the damage consists of linear combination of the normalized values of maximum displacement and hysteretic ene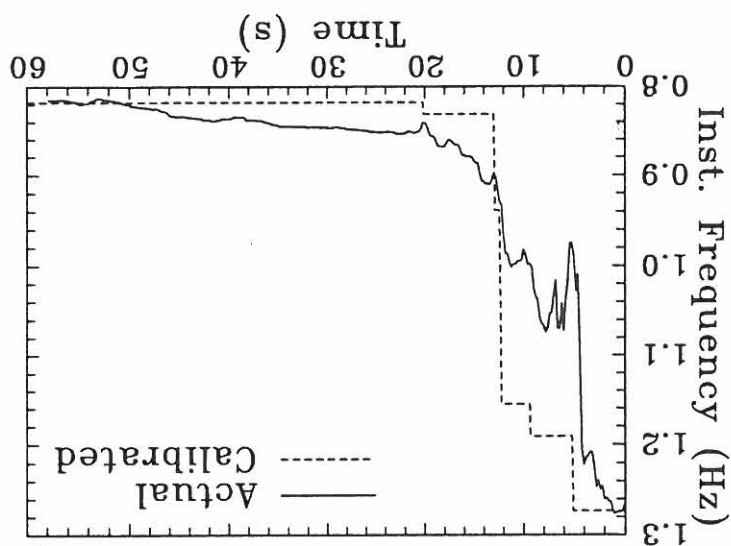rgy dissipated during the excitation, and the collapse is considered to occur when this index attains a value of 1.0 (Park et al. (1987)). This model however requires the estimation of a strength deteriorating parameter, and therefore, damage in this study has been assumed to be measured through the index,

$$DI = \frac{\frac{x_{\max}}{z_{00}} - 1}{\mu - 1} \qquad (7)$$

for simplicity. Here, $x_{\max}$ is the maximum deformation of the oscillator during the excitation and μ is the maximum ductility available with the oscillator. This index gives zero value for $x_{\max} = z_{00}$ and unit value for $x_{\max} = \mu z_{00}$. Since this index does not involve the normalized energy term (besides the recoverable deformation being removed from the normalized displacement term), we arbitrarily assume a lower value of 0.8 for this at collapse. The damage index, DI, can however be used to predict damage in the proposed oscillator model, provided the available ductility is known apriori.

It has been mentioned earlier that the parameter, n, is a measure of ductility available in the system and therefore, it should be related to the parameter, μ. The precise relationship between the two may be estimated if the damages defined by the index, DI, and maximum decrease in the natural frequency of the structure during the excitation are considered

comparable. DiPasquale and Çakmak (1990) have shown that a median value of 69 percent for the maximum decrease in frequency corresponds to the limit state of collapse. By using the equivalence of this damage state with that corresponding to $DI = 0.8$, and by considering the first example case (that of 1994 Northridge Earthquake) for $n = 0.5, 1.0,$ 2.0, 4.0, 6.0, 8.0, 10.0, and 12.0, it has been found that the equation,

$$\mu = 3.44 n^{0.31} \tag{8}$$

accurately describes the relationship between the two ductility parameters. This equation is also found to be applicable for the other two example cases.

Once the damage index, DI, is defined in terms of the parameter, n, it is possible to correlate the strength and stiffness degradation with DI for different damage states in the proposed oscillator. For this purpose, the SDOF oscillator in the first example case has been subjected to different scaled versions of the considered excitations, $\alpha \ddot{u}_g(t)$, $\alpha \in [\alpha_{\min}, \alpha_{\max}]$, where $\alpha_{\min}$ is the maximum value of α for no damage to the oscillator and $\alpha_{\max}$ is the value of α for the damage of 0.8. Reductions in stiffness as fractions of the initial linear stiffness, ω_0, and in yield strength as fraction of the initial strength have been obtained for various damage states corresponding to different values of α in case of $n = 2, 4$ and 6. Figs. 6 and 7 show the so obtained correlations of stiffness and strength reductions
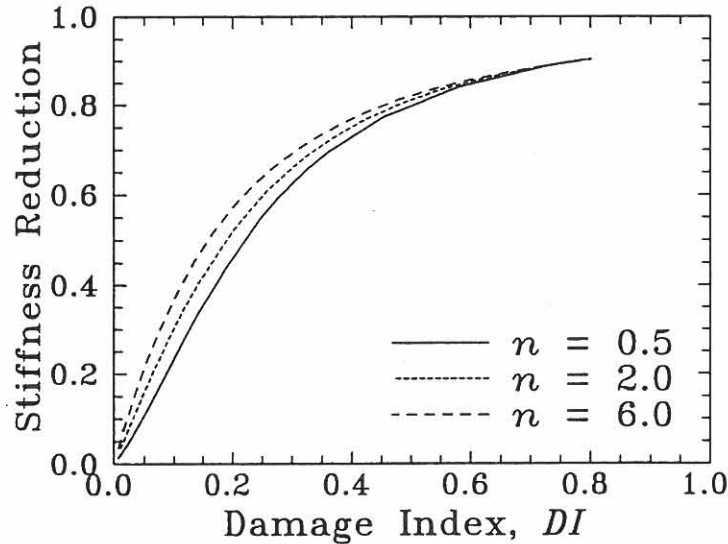
Figure 6 *Correlations of Stiffness Reduction with Damage Index for Different Values of n.*

with the damage index, DI. It may be seen that due to the enforced equivalence of damage states in terms of frequency reduction and DI, all three curves converge to the same value of stiffness reduction, i.e., 0.904 at the $DI = 0.8$. The values of $\alpha_{\max}$ are however different in all three cases, with greater value required to be used for higher n (this means that same damage takes place at a lower magnification for systems with lower ductility, while
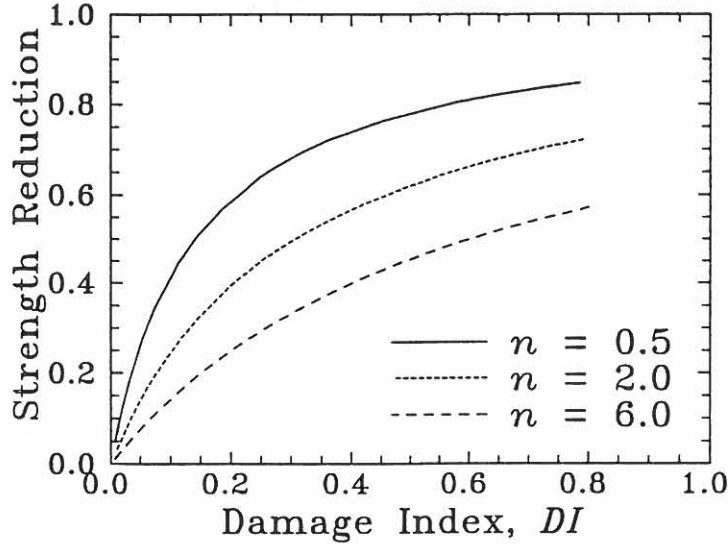
Figure 7 *Correlations of Strength Reduction with Damage Index for Different Values of n.*

initial yield strength is kept unchanged). At other values of DI also, the effect of n is not very significant, even though stiffness reductions are greater for the oscillators with greater ductility supply. It is seen that stiffness reduction is about 70 percent for the moderate repairable damage of 0.4 and 50 percent for the minor damage of 0.2. In case of strength reductions (see Fig. 7), however, the situation is quite different as the value of available ductility makes a substantial difference, with the oscillators with higher ductility exhibiting lesser strength reductions. At the damage state of collapse, strength reduction is as high as 85 percent in case of $n = 0.5$ while that is just 57 percent in case of $n = 6.0$. In this case, therefore, it is important to have a more accurate estimate of the ductility available in the structural system. Fig. 7 also shows that the systems with little ductility supply (say, $\mu < 3$) may have strength reductions of about 55 to 60 percent in case of rather minor damage of 0.2 which may make them quite vulnerable to the effects of aftershocks. This is however true only when the initial yield strength is a constant parameter (we can always reduce the damage by increasing the z_{00} level, irrespective of the available ductility).

It has been observed that considering the second and third example cases and more cases of earthquakes ground motions leads to different sets of $\alpha_{\min}$ and $\alpha_{\max}$, but little difference is made to the correlations presented in Figs. 6 and 7. In view of this, these correlations can be useful as explained in the introduction, subject to the applicability of various underlying assumptions for the proposed oscillator.

In the present design philosophy of providing adequate earthquake-resistance, the damage state of collapse is envisaged for the most critical event expected at the site of the structure. This 'single-event design' philosophy does not account for the effects of aftershocks following the main event on the damage state of structure. In other words, the possibility of structure reaching the collpase state of damage during one of the aftershocks is discounted. This aspect has been overlooked so far possibly due to the lack of reliable information on stiffness and strength degradation following an earthquake event. Since the repair and retrofitting operations on a damaged building usually take a few months to be carried out after the occurrence of the main event, one can take the same initial strength and stiffness for the building during the first aftershock as the final (degraded) values after the main event. Similarly, the final values after the first aftershock can be taken as the initial values for the prediction of damage during the second aftershock.

A preliminary numerical study has been carried out here to appreciate the lack of conservatism associated with the 'single-event design' philosophy. The proposed oscillator has been considered for the same three buildings as considered earlier with $n = 6$ (or, $\mu \approx 6$) and $\zeta = 0.01$. The corresponding oscillators have been subjected to a sequence of ground accelerograms, $\eta \Gamma \alpha_{max} \ddot{u}_g(t)$, $\eta^2 \Gamma \alpha_{max} \ddot{u}_g(t)$, $\eta^3 \Gamma \alpha_{max} \ddot{u}_g(t)$, ..., in case of different free-field acceleration time-histories, $\ddot{u}_g(t)$, and varying values of η between 0.01 and 0.7. In each case of $\ddot{u}_g(t)$ and η, the maximum value of Γ, i.e. Γ_{max}, is determined such that the total cumulative damage during all the aftershocks is less than the limiting value of 0.8 and that the maximum deformation in the structure does not exceed μ times the initial value of yield displacement. It may be seen that the considered sequence of aftershocks corresponds to an exponential decay of peak ground acceleration from one event to the another event. The example free-field accelerograms considered for this study are: (i) N90E component at Nordhoff Avenue Fire station, Arleta, California during the 1994 Northridge earthquake, (ii) S90W component at Civil Center Grounds, Big Bear Lake, California, during the 1992 Big Bear earthquake, (iii) N90E component at 116th Street School, Los Angeles, California, during the 1992 Landers earthquake, (iv) S90W component at Riverside airport, California, during the 1986 Palm Springs earthquake, (v) N90E component at Telegraph Hill, San Francisco, California, during the 1989 Loma Prieta earthquake, and (vi) N90E component at Imperial County Services Building, El Centro, California, during the 1979 Imperial Valley earthquake. The normalized time-histories of these ground motions (to 1.0g peak ground acceleration) are shown in Fig. 8. It may be seen that all six example motions cover a large range of ground motions in terms of frequency content and arrival of different types of waves.

Figs. 9, 10 and 11 show the variations of Γ_{max} with η respectively for Building 1 (i.e., the Van Nuys hotel as in 1994), Building 2 (i.e., Imperial County Services Building), and Building 3 (i.e., the Van Nuys hotel as in 1971), for all six ground motions. In each figure, it is seen that all six curves expectedly approach the value of $\Gamma_{max} = 1$ with η going to zero. Though no definite trend is observed in considering different buildings for a given earthquake, there appears to be a perceptible effect of the type of ground motion. It is

seen that the value of Γ_{max} remains above 0.8, except for very high values of η (which are
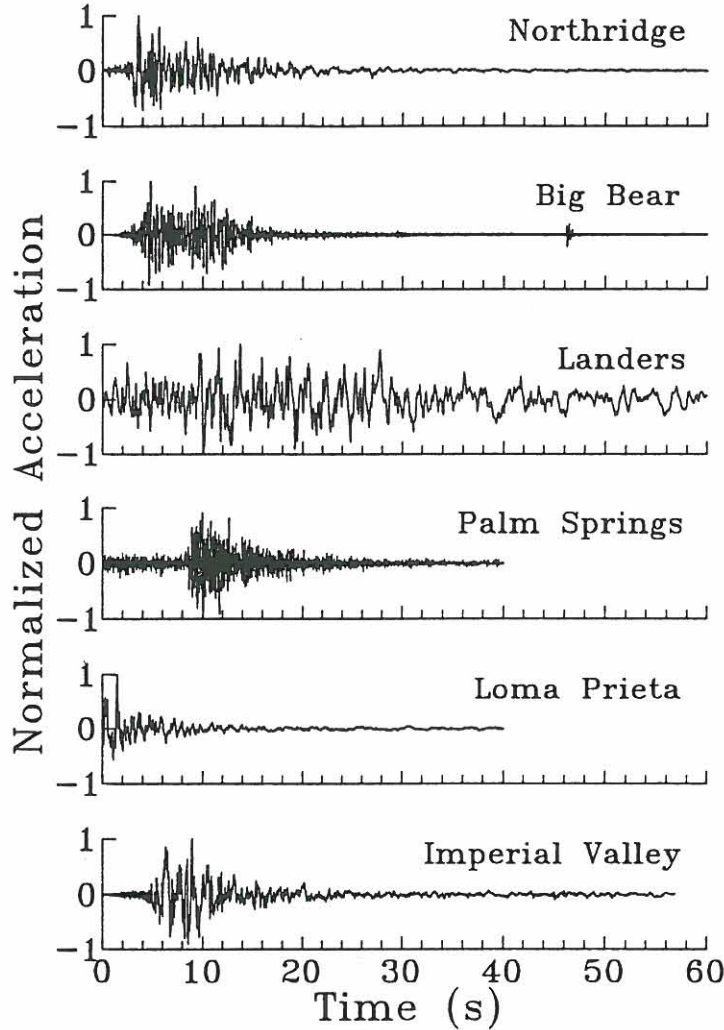

Figure 8 *Normalized Acceleration Time-Histories for the Example Free-Field Motions.*

anyway unlikely), in case of Landers, Palm Springs, and Loma Prieta ground motions. For these ground motions, ignoring aftershocks may not make much difference since a ground motion with the intensity as much as 0.85–0.95 times that of the critical ground motion would be required to cause collapse when the effects of aftershocks are included. In case of another extreme (of low Γ_{max} values) represented by the Big Bear ground motion, a ground motion with about 0.7 times the intensity of the critical motion would cause collapse if it is followed by aftershocks of 0.3, 0.09, ... times the intensity of main shock. Similar is the observation for the Northridge and Imperial Valley motions. For these cases, the structure may thus collapse even if the main event is 30 40 percent less intense than that used for the design calculations. The observed narrow and wide variations in Γ_{max}, respectively, in
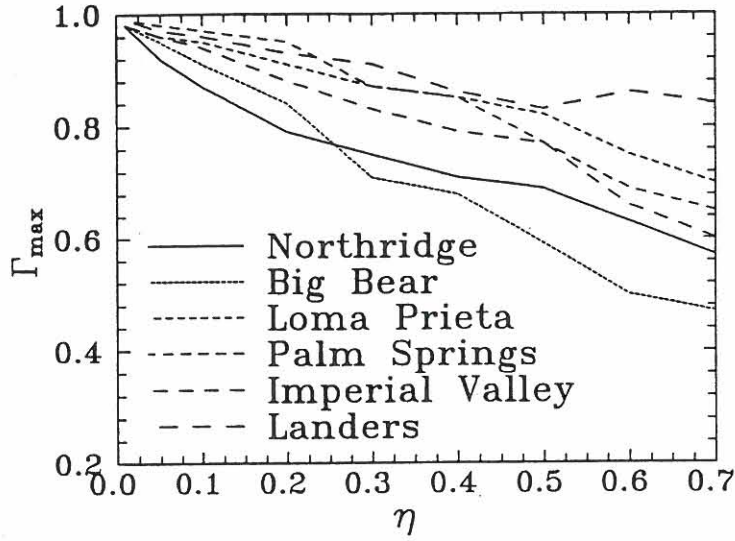
11

Figure 9 *Variations of Γ_{max} with η for Different Example Motions in Case of Building 1 (Van Nuys Hotel as in 1994).*
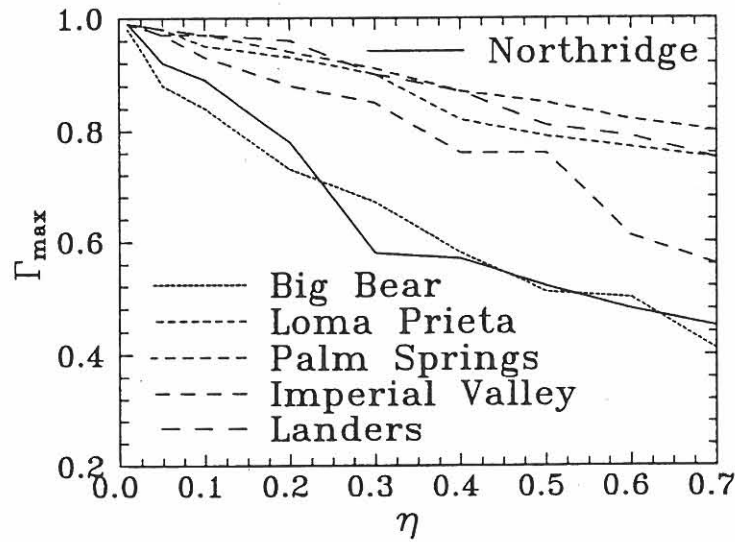

Figure 10 *Variations of Γ_{max} with η for Different Example Motions in Case of Building 2 (Imperial County Services Building).*

case of the Landers and Big Bear motions, as we go from $\eta = 0.01$ to $\eta = 0.7$, correlate well with the durations over which most of the energy arrives. Whereas 90% of the total

12

energy arrives in just 16.2% of the total duration in case of Big Bear motion, it takes 71.7% duration for the same energy to arrive in case of Landers ground motion. In case of Northridge, Palm Springs, Loma Prieta, and Imperial Valley motions, this (percentage) duration is 21.7, 34.8, 23.8 and 21.2, respectively. This means that the motions with the
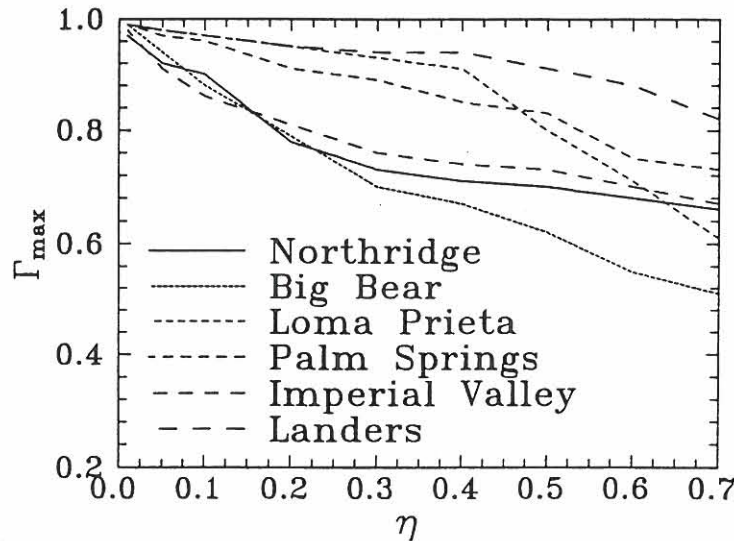

Figure 11 *Variations of Γ_{max} with η for Differe
Motions in Case of Building 3 (Van N
in 1971).*

steepest rate of energy arrival near the occurrence of largest peak (such impulsive motions are usually recorded at small epicentral distances) may be expected to be associated with wider variations in Γ_{max} and thus, with greater role of aftershocks in the collapse of structure. If the results of Figs. 9–11 are interpreted in an alternative way, it may be said that the design yield strength is required to be increased for a structure to survive aftershocks also, and that such an increase may be as much as 72 percent for Building 2 in case of Northridge type of ground motion.

It may be mentioned here that out of the two conditions given above for collapse, the condition of maximum deformation has been found to be governing in all the cases. In view of this, it is unlikely that considering normalized energy term in the damage index will make substantial difference to the above observations. Further, these observations are based on the assumption that the ground motions corresponding to the aftershocks may be represented as scaled versions of that corresponding to the main event. This assumption may be acceptable as long as the mechanism of energy release at other parts of the active fault is similar to that for the main event. Since the total durations of the aftershocks may often be less due to smaller energy release, these observations need to be investigated further through a more realistic modelling of the aftershocks.

CONCLUSIONS

The well-known Clough-Johnston oscillator has been modified to account for strength degradation in case of elasto-plastic oscillators. This oscillator is simple as it uses yield displacement level and a ductility supply-related parameter as inputs. It can be suitably calibrated within an expected range of available ductility to accurately model the observed softening during an earthquake ground motion.

The proposed oscillator has been calibrated in case of two buildings which suffered heavy damages during the 1971 San Fernando, 1979 Imperial Valley and 1994 Northridge earthquakes, and the calibrated oscillator has been used to estimate the correlations of stiffness and strength degradations with damage. It is hoped that these correlations will be useful to the engineering community involved in the post-earthquake operations till more reliable estimates become available from more detailed analyses.

Based on the assumption that the ground motions during aftershocks can be represented as the scaled-down versions of those during the main shocks and by using the proposed oscillator, a preliminary numerical study has shown that neglecting aftershocks in the cases of ground motions with large energy arrivals in shorter durations may be unconservative.

ACKNOWLEDGEMENTS

REFERENCES

Clough, W. and S.B. Johnston (1966). Effect of stiffness degradation on earthquake ductility requirements, *Proc. 2nd Japan Earthq. Symp.*, 227–232.

DiPasquale, E. and A.S. Çakmak (1990). Detection of seismic structural damage using parameter-based global damage indices, *Probab. Emg. Mech.*, 5, 60–65.

Kirkegaard, P.H., P.S. Skjærbæk, and P. Andersen (1996). Identification of time varying civil engineering structures using multivariate recursive time domain models, *Proc. ISMA21, Leuven*, 1337–1348.

Köylüoğlu, H.U., S.R.K. Nielsen, A.S. Çakmak, and P.H. Kirkegaard (1997). Prediction of global and localized damage and future reliability for RC structures subject to earthquakes, *Earthq. Eng. Struct. Dyn.*, **26**, 463–475.

Minai, R. and Y. Suzuki (1985). Seismic reliability analysis of building structures, *Proc. ROC-Japan Joint Seminar on Multiple Hazards Mitigation, National Taiwan University, Taiwan ROC*, 193–207.

Park, Y.-J. and A.H.-S. Ang (1985). Mechanistic seismic damage model for reinforced concrete, *J. Struct. Eng. (ASCE)*, **111(4)**, 722–739.

Park, Y.-J., A.H.-S. Ang, and Y.K. Wen (1987). Damage-limiting aseismic design of buildings, *Earthq. Spectra*, **3(1)**, 1–26.

15